Eur Biophys J (2009) 38:159–173
DOI 10.1007/s00249-008-0364-2

ORIGINAL PAPER

Calcium and the role of motoneuronal doublets in skeletal muscle control

Bjørn Gilbert Nielsen

Received: 30 May 2008 / Revised: 5 August 2008 / Accepted: 5 August 2008 / Published online: 27 August 2008

Abstract This work presents a novel structural model of skeletal muscle activation, providing a physiologically based account of frequency-dependent muscle responses like the catch-like effect. Numerous Ca^{2+} reservoirs within muscle fibers are considered, and a simplified analysis of the allocation of Ca^{2+} resources and the dynamics of calcium transport is proposed. The model correctly accounts for catch-like effects in slow and fast-twitch fibers during long-train stimulations and force–frequency relations in different muscle types. Results obtained from the model compare favorably to experiments showing that prolonged increases in force characteristic of the catch-like effect are not accompanied by sustained increases in free myoplasmic Ca^{2+}. Also, in agreement with early experiments, the interspike interval in catch-inducing doublets is seen to be an important parameter for regulating the precise onset amplitude of the catch-like effect. This suggests that a plausible physiological function for the inclusion of doublets or the exclusion of individual spikes within a regular motor-neuronal spike-train is to rapidly bring skeletal muscles to predefined target forces according to prespecified motor programs in the central nervous system. This is a potentially very useful property directly mediated by the catch-like process modeled here. One further prediction of the model is that the slope of the frequency–tension profile of a given muscle is highly sensitive to changes in the efficiency and temporal characteristics of the dihydropyridine–ryanodine receptor complex. Interestingly, this is consistent with findings made on cardiac muscles, and might incidentally explain some instances of cardiac failure.

Keywords Excitation–contraction coupling · Motoneuronal doublets · Force–frequency relation · Preprogrammed muscle activation

B. G. Nielsen (✉)
Quantum Protein Centre (QuP), Department of Physics,
Technical University of Denmark, Bldg. 309,
2800 Lyngby, Denmark
e-mail: bjorn.nielsen@fysik.dtu.dk; bnielsen@fysik.dtu.dk

Introduction

While stimulating muscle fiber preparations from the triceps surae muscle of a cat, Burke et al. (1970) observed that the addition of an extra pulse in an otherwise regular pulse-train consistently led to a prolonged increase in muscle force. This so-called "catch-like" effect is frequency and motor-unit type dependent but has been shown to be independent of the neuromuscular junction and is now considered an intrinsic property of all skeletal muscle tissue. The exact mechanism whereby the catch-like property is brought about is still much discussed [see Binder-Macleod and Kesar (2005) for a recent review]. This topic has gained renewed importance, thanks to the observation of double discharges, or "doublets" [as defined by Simpson (1969)] during in vivo motor neuron firing sequences, which presumably could elicit such catch-like muscle responses [see, e.g., Maton and Bouisset (1975), Søgaard et al. (2001), and review by Garland and Griffin (1999)]. As will be shown in this work, the nervous system could in principle take advantage of such catch-inducing doublets to produce precisely timed jumps in muscle tension, simply by changing the interspike interval of the doublet [in agreement with experiments reported in Maton and Bouisset (1975)].

Additionally, in the hope of helping patients with spinal cord injuries or otherwise reduced muscle strength, much

research has focused on defining pulse sequences that optimize the force produced by muscles during functional electrical stimulation (FES) (Stein and Parmiggiani 1979; Talonen et al. 1990; Mourselas and Granat 1998; Ding et al. 2000; Kebaetse et al. 2001, 2005). Early studies suggested that the catch-like effect might be invoked to this end (Binder-Macleod and Barker 1991), the main rationale here being, to produce activation sequences that avoid the induction of fatigue in muscle while maximizing force. Some experimental evidence in support of this approach was recently reported by Shimada et al. (2006).

In recent years, a number of muscle activation models have been presented that to some extent account for the catch-like effect (see, e.g., Hannaford 1990; Chou and Hannaford 1992; Otazu et al. 2001) or claim to be accurate models of the frequency-dependent responses of muscle (Wexler et al. 1997; Ding et al. 1998). An early phenomenological model by Hannaford (1990) gave reasonable results but provided little physiological detail, and no attempt was made by the author to relate the suggested state variables to physiology. A more advanced model was proposed by Chou and Hannaford (1992), which did a much better job at capturing the physiological processes in muscle tissue leading to frequency-dependent muscle activation patterns. In that model, two stable equilibrium points associated with the binding of Ca^{2+} to troponin were proposed to be the origin of the catch-like effect, but no physiological evidence was provided for this. Furthermore, the model requires the specification and fitting of a large number of parameters and state variables, which are not easily measured, making it cumbersome and perhaps of limited use.

In a model proposed by Otazu et al. (2001), the claim is made that post-tetanic potentiation (PTP) and the catch-like effect share a common origin, and is based on the existence of multiple equilibrium points for calcium concentration within the myoplasm. The model includes a detailed description of calcium binding/unbinding to different proteins and includes a detailed (Michaelis–Menten type) model of the sarco(endo)plasmic Ca^{2+}-ATPase (SERCA). From this model, it is difficult to see which parameters are crucial for eliciting the catch-like effect, especially considering that extensive parameter adjustments were required. Besides, the proposed existence of multiple equilibrium points for myoplasmic $[Ca^{2+}]$ is at odds with recent experimental findings reported by Abbate et al. (2002) defending the view that prolonged force increases are not *in general* due to increased myoplasmic $[Ca^{2+}]$. In muscles receiving adrenergic stimulation, PTP has been observed in association with increased resting myoplasmic $[Ca^{2+}]$, as reported by Decostre et al. (2000). Also Cannell (1986) reports prolonged increases in myoplasmic $[Ca^{2+}]$, but the duration of these is in the range of seconds and are thus too short to account for PTP. Most of the experimental evidence cited by Otazu et al. (2001) in favor of assuming a prolongued increase of myoplasmic $[Ca^{2+}]$ (Lee et al. 1991; Westerblad and Allen 1993; Edman 1996) is more related to Ca^{2+} increases during muscle fatigue, not PTP, and tend to point to the conclusion that a prolonged increase of myoplasmic $[Ca^{2+}]$ often is the hallmark of fatigue.

In work by Wexler et al. (1997), another model of frequency-dependent muscle responses was developed. This model required fewer parameters, but not without problems: close inspection of their parameter list [Table II in Wexler et al. (1997)] reveals that some of these parameters when fitted to different experimental subjects did vary by up to three orders of magnitude even within the same type of muscle, casting some doubt on the appropriateness of the parameters selected for optimization. Furthermore, Wexler et al. (1997) concede that their model failed to reproduce muscle forces during long-train stimulations at some frequencies. Some of the early problems were amended in later work (Ding et al. 2000, 2002; Chou et al. 2005). However, in all their models, a strong dependence on the force-producing apparatus is required. Given that only isometric contractions were considered, a simple force generation model was used to derive the model, namely Maxwell's three-component model consisting of a spring, a damper and a motor in series (Wexler et al. 1997). It is therefore unclear how well their model would fit data if more realistic Huxley-type muscle force models were used instead, or simply if the movement were not isometric. Furthermore, these models have the disadvantage that they require prespecification of the full activation sequence to optimize the parameters to that particular sequence. This is of course very useful when trying to predict pregenerated optimal electrical stimulation sequences, but is of little use when considering the task of analyzing and/or reproducing real-time behavior with continuous and highly varying spike sequences. In this context, it would be an advantage to develop a model that does not depend on prespecified sequences, but that can respond continuously to any activation sequence. Given these caveats, it seems more useful to keep the actual force-producing mechanisms mathematically separate from the Ca^{2+} activation dynamics so that different muscle-force models and Ca^{2+} activation models in principle may be tested independently. At present, this simplified approach will be adequate to describe the dynamics related to the catch-like effect in skeletal muscle. In essence, this simplification step is taken for several reasons. First, given the timeframe of the modeled phenomena (the catch-like effect, which lasts for seconds and minutes), such a simplification leads to a much clearer and simpler description of the involved dynamics. Second, it allows us to first identify the main elements and

then home in on the particulars. Third, it allows for a modular approach, where interdependences (such as feedback between modules) can be described in simple terms once known. Thus, starting from such a strict separation of terms, further improvements and additions to the model should be straightforward. It might even be easier to identify and formally describe and incorporate structural elements that in muscles are responsible for phenomena such as the possible feedback between tension and Ca^{2+} binding, and cooperative effects in the thin filaments involving multiple binding states [as discussed by Geeves and Lehrer (2002)] or even reaction rates and binding affinities that depend on muscle tension.

Through the models reviewed here it is seen that there are many very different ways of obtaining the same dynamics in a system as complex as the muscle cell. From a biophysical point of view, it is often best to start with as simple a model as possible that consists of very few and easily measurable variables that have a clear relationship to observable quantities. Once these variables are known and the overall dynamics understood, further work may be done to elucidate the true (often molecular) origin of these variables. For example, by using spectroscopic methods, it is straightforward to directly measure the time-constants governing Ca^{2+} reuptake through the SERCA channel (Gilchrist et al. 1997), a parameter that may easily be included in an excitation–contraction model, and is in fact sufficient as we shall see later [although detailed molecular models of SERCA (Higgins et al. 2006) and other Ca^{2+} transporters are important additions that might be considered in future versions of the model]. Furthermore, to compare systems that presumably share similar underlying mechanisms but present highly divergent dynamic behaviors—as is the case between slow, fast, smooth and cardiac muscle fibers—a model should aim at being general enough to capture the effects under study in as wide an array of different systems as possible, perhaps even suggesting a continuum between these categories. For example, by failing to explicitly include variables for setting the force–frequency relation of individual muscle fibers, a determining factor for their classification, previous models have been limited to very specific and already well characterized muscle samples. Thus, in spite of the fact that all of the models mentioned previously make good headway toward understanding muscle activation-related nonlinearities like the catch-like effect, they do have several shortcomings, and leave open the very pertinent question: which are the essential variables that dictate muscle activation dynamics?

To answer this question, it is helpful to make a clear distinction between the relatively fast *forward* Ca^{2+} dynamics describing Ca^{2+} release mechanisms promptly leading to muscular contraction, and the much slower *backward* Ca^{2+} dynamics involving the recovery (reuptake) of Ca^{2+} to the stores from where it was initially released. The basic tenet here is that release mechanisms in general (be they of ions like Ca^{2+} or large molecules like neurotransmitters) are optimized for speed and are often much faster than the corresponding reuptake mechanisms. When considering dynamics at the cellular scale, release delays are so short that they may often be assumed to be instantaneous, purportedly contributing little to long-term dynamical phenomena like the catch-like effect. This is especially so considering the 10 ms time scope that is relevant for skeletal muscle stimulation (depending on type, muscles become tetanized at 50–120 Hz). The end result is a model that captures the essence of the skeletal muscle cell's Ca^{2+}-dynamics but with a minimal number of parameters, because only relatively "slow" time constants are considered.

One major goal of the present work has been to develop a model of skeletal muscle activation that has fewer parameters and is easier to parametrize than previous models, with the aim to interpret and extrapolate data generated from long spike trains during experimental or clinical situations where in vivo nerve and muscle stimulations take place. Very few and quite simple measurements are required to calibrate the present model to a particular muscle activation experiment. As will be shown, the most significant parameters are related to the time constants for Ca^{2+} removal from the myoplasm. Such time constants are easily accessible via the use of Ca^{2+} indicators in vivo, bearing in mind the potentially very strong influence that Ca^{2+}-binding indicators may have on the dynamics of the studied system by limiting the diffusion of calcium. Further constraints on the model parameters may be obtained simply by measuring the force–frequency relationship of a muscle, because as it turns out, the slope of this relationship is controlled by a single parameter in the model (involved in the interaction between the dihydropyridine receptor and the ryanodine receptor). Thus, with two simple routine measurements, the present model may be brought within the dynamic range of the muscle fibers under investigation, whether they be slow or fast muscle fibers.

Methods for modeling Ca^{2+} dynamics in the muscle fiber

The importance of Ca^{2+} for muscle contraction has been clearly established (Ebashi and Endo 1968). Movement of Ca^{2+} between different compartments of the cell is the key to understanding muscular contraction, and the precise dynamics of Ca^{2+} transport will dictate how the cell behaves in response to stimulation. Capturing such

dynamics requires clarification of the time constants involved and the distribution of calcium within the muscle cell's many compartments. The following is a brief review of the most important aspects with a clear emphasis on transport direction of Ca^{2+}. The main conclusions are summarized in Fig. 1.

Ca^{2+} release—fast forward dynamics

The arrival of an action potential to the neuromuscular junction and the subsequent release of acetylcholine (ACh) leads to a postsynaptic depolarization, the so called end-plate potential, which may trigger an action potential to rapidly propagate over the surface of the corresponding muscle fiber. This propagating action potential is then conducted into the innermost regions of the individual muscle fibers via a system of transverse tubules (T-tubules), the depolarization of which leads to the opening of voltage-gated Ca^{2+} channels embedded into the membrane of the sarcoplasmic reticulum. The exact details of this process are still debated, but the current consensus is that voltage sensitivity is mediated by dihydropyridine receptor (DHPR) channels in the T-tubule membrane [for review, see Franzini-Armstrong (1999) and Dulhunty et al. (2002)], and Ca^{2+} release is mediated through membrane-bound ryanodine receptors (RyR, with subtypes RyR1 and RyR2) in the termini of the sarcoplasmic reticulum [reviewed by Fill and Copello (2002)] in close collaboration with calsequestrin [see review by Beard et al. (2004)]. There is a functional coupling between DHPR and RyR, which depends on the type of muscle tissue [see reviews by Bottinelli and Reggiani (2000) and Dulhunty et al. (2002)]. In cardiac muscle, the opening of DHPR leads to influx of extracellular Ca^{2+}, inducing RyR2 to open and thus permit release of Ca^{2+} from the sarcoplasmic termini (where calsequestrin acts as a Ca^{2+} buffer) into the myoplasm, i.e. the intracellular regions of the sarcomere where the myosin and actin filaments are located. In skeletal muscle, there appears to be a more direct physical coupling between DHPR and RyR1, essentially entailing that the RyR1 Ca^{2+} channel opens in response to conformational modifications in loop II/III regions of DHPR that are induced by membrane voltage changes [some of the details concerning this interaction have been elucidated by Nakai et al. (1996), Gurrola et al. (1999), Protasi et al. (2002) and Kugler et al. (2004)]. In either case, the final event causing contraction in muscle is the release of Ca^{2+} ions into the myoplasm, and the binding of these to troponin C (TnC) in what appears to be a quite fast process (Johnson et al. 1979). The thus activated TnC weakens the bond between troponin I and actin, allowing tropomyosin (which is indirectly bound to troponin I via troponin T) to slip back into its normal

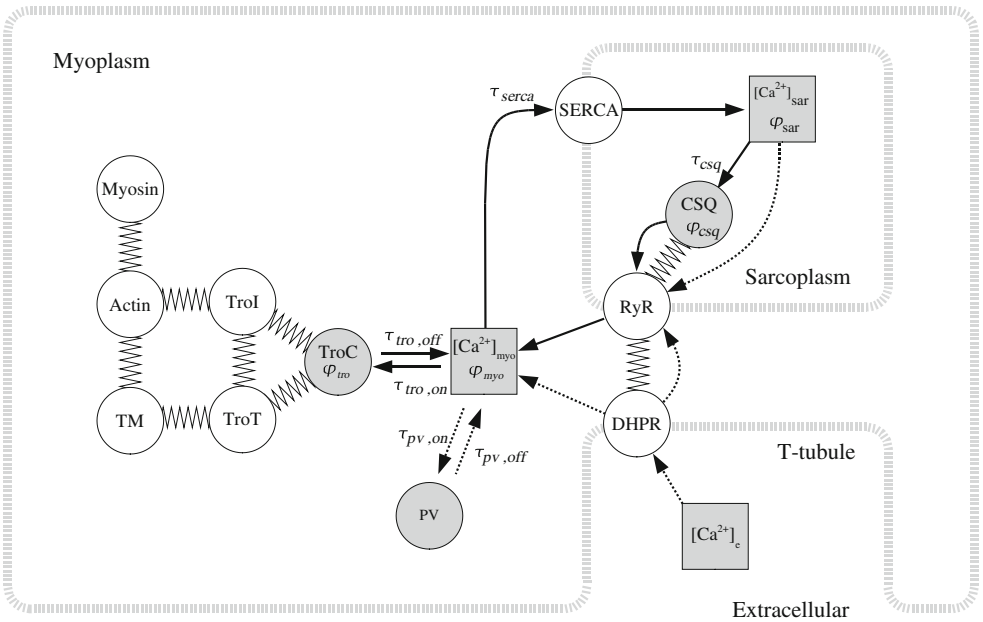

Fig. 1 Conceptual diagram of a simplified interaction network for Ca^{2+}. *Circles* denote a few of the main proteins involved in the excitability–contraction coupling. *Squares* indicate free Ca^{2+} dissolved in the fluids corresponding to the different membrane systems: myoplasm, sarcoplasm and extracellular. Areas shaded in *gray* indicate loci where Ca^{2+} spends most of the time, and correspond to the different Ca^{2+} fractions given in the model. The *zig-zagging lines* connecting *circles* indicate physical interactions between the proteins, and *arrows* show the main flow of Ca^{2+} throughout the system (*dashed arrows* are not considered in the present model except for the case of parvalbumin). Time-constants (τ) are as indicated in the text. *CSQ* calsequestrin, *DHPR* dihydropyridine receptor, *RyR* ryanodine receptor, *SERCA* sarco(endo)plasmic reticulum calcium ATPase, *TroC* troponin C, *TroI* troponin I, *TroT* troponin T, *TM* tropomyosin, *PV* parvalbumin. Variables as defined in text

position, finally revealing the actin–myosin binding sites and allowing the production of force [a clearly illustrated description of this process is given by Alberts et al. (2002)].

Ca^{2+} recovery—slow backward dynamics

According to Collins et al. (1973), fast-twitch skeletal muscle troponin C has four binding sites for Ca^{2+}, two with a high affinity for Ca^{2+} and two with a low affinity for Ca^{2+}. According to Potter and Gergely (1975), it is the later two that are the regulatory sites for muscle contraction [see also review by Collins (1991)]. It is interesting to note that the properties of TnC may vary depending on the type of fiber; for example, it has been observed that in cardiac muscle one of the low-affinity Ca^{2+} sites on TnC has lost its ability to bind calcium (van Eerd and Takahashi 1975), evidently affecting the association and dissociation time constants [for further distinctions, see also review by Bottinelli and Reggiani (2000)]. However, Kerrick et al. (1976) concludes that differences in Ca^{2+} binding affinity to troponin in fast and slow-twitch muscle alone cannot fully account for the different sensitivities of these muscles to Ca^{2+}.

After Ca^{2+} dissociation from troponin, the tropomyosin molecule will again conceal the actin-binding sites as the Ca^{2+} concentration lowers. From the myoplasm, Ca^{2+} is continuously sequestered back into the sarcoplasm by the sarco(endo)plasmic reticulum Ca^{2+} ATPase (SERCA), a membrane bound ion pump. Mention should also be made of another important Ca^{2+} sink that is present exclusively in the myoplasm of fast-twitch muscle fibers, namely the Ca^{2+}-binding protein parvalbumin (see Fig. 1), which has been suggested to account for the fast relaxation times achieved by type II fast-twitch muscles (Celio and Heizmann 1982).

There is an uneven distribution of SERCA and RyR channels within the sarcoplasmic reticulum, the former protein being concentrated along the longitudinal segments of the SR (Jorgensen et al. 1979, 1982), whereas the latter is mostly concentrated within the terminal cisternae [also reviewed in Takekura et al. (2001)]. Thus, reuptake of Ca^{2+} via SERCA occurs at a location that is far removed from where Ca^{2+} is initially released through RyR. This potentially results in a transmission delay that corresponds to the time it takes for Ca^{2+} to diffuse the corresponding distance. This delay is normally not observed, thanks to the activity of calsequestrin (CSQ), a low-affinity high-capacity Ca^{2+} buffer that is found in the terminal cisternae of the SR (Jorgensen et al. 1979, 1983) in close proximity to the RyR channels [reviewed in Beard et al. (2004)]. Although it has been shown under certain circumstances that some invertebrate muscles may function even without CSQ [*C. elegans*; see Cho et al. (2000)], consensus is that normal skeletal muscle function requires CSQ to buffer Ca^{2+} to release it when RyR becomes active, and furthermore, it is thought that CSQ forms links to RyR and thus itself participates in regulating RyR function (Murray and Ohlendieck 1998).

Model equations

During normal muscle function (no fatigue, no tetanic potentiation), Ca^{2+} moves in a closed circuit so the total amount of Ca^{2+} within a cell during a short burst of activity is here assumed to remain relatively constant—no new calcium is added to or removed from the intracellular milieu of the muscle cell—at least to a first approximation. However, at all times, calcium will be distributed inhomogeneously throughout the cell, and variable fractions of calcium (φ) will be concentrated at different loci depending on the recent activation history of the cell. Relevant to the present study, it will be assumed that calcium may be found in any of the following fractions (see Fig. 1):

φ_{myo}	Free calcium in the myoplasm
φ_{sar}	Free calcium in the longitudinal regions of the sarcoplasm
φ_{csq}	Calcium bound to calsequestrin or in the sarcoplasmic terminal
φ_{trc}	Calcium bound to troponin C
φ_{par}	Calcium bound to parvalbumin

The total amount of calcium available to the cell is then $\varphi_{tot} = \varphi_{myo} + \varphi_{sar} + \varphi_{csq} + \varphi_{trc} + \varphi_{par}$ (and may be set equal to one for normalization purposes). Note that $\varphi_{par} = 0$ in slow-twitch fibers. Movement of Ca^{2+} between these reservoirs is not instantaneous, but when considering the relatively slow dynamics of the catch-like effect, only six time constants are considered rate limiting in the present model:

τ_{csq}	Time constant for diffusion and calsequestrin governing $\varphi_{sar} \rightarrow \varphi_{csq}$
τ_{serca}	Time constant for SERCA governing $\varphi_{myo} \rightarrow \varphi_{sar}$
$\tau_{trc,on}$	Binding time constant for troponin C governing $\varphi_{myo} \rightarrow \varphi_{trc}$
$\tau_{trc,off}$	Dissociation time constant for troponin C governing $\varphi_{trc} \rightarrow \varphi_{myo}$
$\tau_{par,on}$	Binding time constant for parvalbumin governing $\varphi_{myo} \rightarrow \varphi_{par}$
$\tau_{par,off}$	Dissociation time constant for parvalbumin governing $\varphi_{par} \rightarrow \varphi_{myo}$

It should be noted that these time constants are not indicative of the time or rate constants for the individual Ca^{2+}-binding proteins as such, but rather reflects the overall Ca^{2+} transport rate between different Ca^{2+}

reservoirs mediated by a large number of such proteins. In fact, in several cases, the involved proteins have turnover rates that are much too slow to directly account for the rapid Ca^{2+} transients that they cause. For example, although the individual SERCA channel has a turnover rate in the order of only 6–36 s^{-1} at 37°C, only 50 ms are required to reduce cytoplasmic [Ca^{2+}] from 10 μM during contraction to 0.1 μM during rest (Peinelt and Apell 2004), corresponding to a time constant of approximately 10–15 ms. This requires a very high density of channels, even up to 30,000 μm^{-2} (Franzini-Armstrong and Ferguson 1985). The corresponding time constants in smooth muscles have been measured to be above 400 ms (Ganitkevich 1999); so, muscles show a wide range of values.

To calculate the time and rate constants directly, one would have to know the precise concentration (or surface density) of Ca^{2+}-binding proteins in a given volume (or membrane area) within a specified type of muscle (e.g., the density of SERCA in the membrane surrounding the sarcoplasm of fast fibers). In addition, it would be necessary to measure the conductance or the rate constant (Ca^{2+} transport rate) for the individual protein. Overall, this would give a total rate constant, k_{Ca}, for the sequestration of Ca^{2+} into a given reservoir. Assuming simple first-order kinetics, we obtain the rate equation $d[Ca]/dt = k_{Ca}[Ca]$, with half-life $t_{\frac{1}{2}} = \ln 2/k_{Ca}$. The time constants used in this work are defined as $\tau = 1/k_{Ca}$.

The first step in the model is to describe Ca^{2+} release in response to an incoming pulse. By the above definitions, φ_{csq} represents the fraction of Ca^{2+} currently present within the terminal cisternae of the SR, and hence readily available for release. Assuming quantal release (similarly to other membrane systems), when a pulse arrives, only a fraction of the recovered Ca^{2+} in φ_{csq} is used, here represented by the release efficiency of the ryanodine receptor, ξ_{RyR}. Formally:

$$\frac{d\varphi_{csq}}{dt} = \frac{\varphi_{sar}}{\tau_{csq}} - \xi_{RyR} \cdot \varphi_{csq} \cdot \delta(t - t_p) \quad (1)$$

where τ_{csq} represents the time constant for recovering Ca^{2+} from the longitudinal segments of the SR back into φ_{csq}. A delta function, $\delta(t-t_{AP})$, relates current time, t, and the time for the arrival of a pulse, t_p [note that $\delta(t-t_p) = 1$ for $t = t_p$, but evaluates to zero otherwise]. After release from the SR terminals, Ca^{2+} directly enters the myoplasm, thus increasing the myoplasmic Ca^{2+} fraction, φ_{myo}, by the corresponding amount (see Fig. 1):

$$\frac{d\varphi_{myo}}{dt} = -\frac{\varphi_{myo}}{\tau_{serca}} - \frac{\varphi_{myo}}{\tau_{trc,on}} + \frac{\varphi_{trc}}{\tau_{trc,off}} + \xi_{RyR} \cdot \varphi_{csq} \cdot \delta(t - t_p) \quad (2)$$

From the myoplasm, Ca^{2+} is continuously sequestered back into the longitudinal segments of the SR via the SERCA pump with a time constant of τ_{serca}. Before reaching the sites where the SERCA pumps are most concentrated, the released Ca^{2+} must first diffuse through the myoplasm where some of it will be taken up by troponin C with binding time constant $\tau_{trc,on}$. Ca^{2+} unbinding from troponin C takes place at a rate defined by the time constant $\tau_{trc,off}$ (see also Fig. 1). The fraction of Ca^{2+} bound to troponin is governed by the following equation:

$$\frac{d\varphi_{trc}}{dt} = \frac{\varphi_{myo}}{\tau_{trc,on}} - \frac{\varphi_{trc}}{\tau_{trc,off}} \quad (3)$$

Finally, the sarcoplasmic fraction of Ca^{2+} depends on the reuptake from the myoplasm through the SERCA pump. Note also that Ca^{2+} in the sarcoplasm is continuously transported to the SR termini and sequestered by CSQ.

$$\frac{d\varphi_{sar}}{dt} = \frac{\varphi_{myo}}{\tau_{serca}} - \frac{\varphi_{sar}}{\tau_{csq}} \quad (4)$$

To a first approximation, the release fraction ξ_{RyR} may be held constant at a small value, but it adds much flexibility to the model if ξ_{RyR} is allowed to vary slowly in response to activation history. These variations would correspond to changes in the efficiency of the DHPR–RyR complex, for example, as a function of the accumulation of calcium in the neighborhood of RyRs. The following scheme has been used for its description:

$$\frac{d\xi_{RyR}}{dt} = -\frac{\xi_{RyR} - \xi_0}{\tau_{RyR}} + \epsilon \cdot (1 - \xi_{RyR}) \cdot \delta(t - t_p) \quad (5)$$

where τ_{RyR} is the time constant associated with the facilitation process, ξ_0 is the initial (and baseline) release efficiency and ε determines the (small) constant amount by which ξ_{RyR} is allowed to change for every presynaptic spike.

To account for the activation dynamics of fast-twitch muscle fibers, the fraction of Ca^{2+} bound to parvalbumin, φ_{par}, may be defined as

$$\frac{d\varphi_{par}}{dt} = \frac{\varphi_{myo}}{\tau_{par,on}} - \frac{\varphi_{par}}{\tau_{par,off}} \quad (6)$$

where $\tau_{par,on}$ is the binding time constant for parvalbumin and $\tau_{par,off}$ is the dissociation time constant. Furthermore, the following modifications should be made to the fraction of Ca^{2+} present in the myoplasm, φ_{myo}: the amount $\frac{\varphi_{myo}}{\tau_{par,on}}$ should be substracted and the amount $\frac{\varphi_{par}}{\tau_{par,off}}$ should be added to the right hand side of (2).

The sarcoplasmic reticulum in muscle cells may be conceptualized as an "internalized" synapse that uses Ca^{2+} as its transmitter in response to the arrival of a pulse through the T-tubule; so, a simple resource allocation model as the one developed here will suffice to describe the movement of Ca^{2+}, and thus to the development of the

catch-like effect. In fact, the approach adopted here was inspired from a resource allocation-based dynamic synapse model developed by Tsodyks and Markram (1997) and Tsodyks et al. (1998) to describe central synapses. However, there are of course many differences although the dynamics might be somewhat similar.

It has been suggested that a link exists between Ca^{2+}-binding affinity to muscle proteins like troponin C and muscle contraction velocity and/or length (Ridgway and Gordon 1975; Brandt et al. 1980; Gordon and Ridgway 1987); however, this has not been modeled here given that only isometric contractions are considered at present, and in view that Patel et al. (1997) have demonstrated an invariance of Ca^{2+} binding to troponin as a function of sarcomere length [see also discussion in Stein et al. (1988)]. However, should one wish to include a velocity or length effect into the model; this could be made to affect the binding/detachment time constants of Ca^{2+} to troponin C.

A further simplification of this model has been to exclude the inverse dependency of Ca^{2+} reuptake to luminal [Ca^{2+}] reported elsewhere (Mogami et al. 1998; Solovyova et al. 2002). The assumption being that, as long as the sarcoplasmic lumen does not become depleted, such effects will be modest. In the present model, even in the presence of high activation levels, the myoplasmic and sarcoplasmic [Ca^{2+}] changes only a few percent (see, e.g., Fig. 5a).

In its present form, this model is entirely based on the flow of Ca^{2+} between different locations with focus on the availability of actin-binding sites provided by activation of the troponin/tropomyosin complex. All the reported results are completely independent of any particular force model, as they are generated directly from the fraction of Ca^{2+} bound to troponin C, φ_{trc}, normalized with respect to this fraction during tetanic activation (50–120 Hz depending on muscle type). This yields a normalized "activation" value, $\overline{\varphi_{trc}}$, which directly can be used to scale the number of active crossbridges, or the fraction of tetanic force. However, there are several options available to obtain the muscle force per se, the simplest being to consider the fraction of Ca^{2+} bound to troponin C, φ_{trc} and use this value in a simple sigmoidal force–calcium relationship (Ebashi and Endo 1968; Kerrick et al. 1976; Brandt et al. 1980; Ridgway et al. 1983; Stein et al. 1988; Abbate et al. 2002). Alternatively, such troponin "activation" values may be used as input to Hill-type muscle models (Hill 1938), spring-damper-actuator models (Chou and Hannaford 1992; Wexler et al. 1997), isometric "filtering" models (Bobet and Stein 1998), linear-spring-based Huxley-type models (Huxley and Simmons 1971) or nonlinear molecular tension-based Huxley-type models (Nielsen 2002a) [used in a preliminary study by Nielsen (2004)]. As discussed by Winters (1995), the actual force model will ultimately depend on the purpose of the modeling as such.

Results

In the following, results will be shown not as actual forces but as muscle activation levels, $\overline{\varphi_{trc}}$, here defined as the current fraction of Ca^{2+} bound to troponin normalized with respect to the corresponding fraction during tetanic activation (50–120 Hz). This activation value can be used directly in a muscle-force model to produce the actual corresponding muscle forces (as demonstrated in Fig. 3, see description below). However, given the nearly sigmoidal steady-state force–calcium relationship mentioned earlier (Ebashi and Endo 1968), it is expected that most of the time the activation value expressed by $\overline{\varphi_{trc}}$ would simply be proportional to the corresponding muscle force (see below). Catch-like dynamics are obtained very directly with this model without the need for a detailed parameter tuning. To allow the model to correspond to different muscle types and preparations, parameter selection was based on rough estimates from the literature and on the constraints imposed by comparison with published muscle twitch experiments [mainly Burke et al. (1976) and Abbate et al. (2002)]. Raw data from Abbate et al. (2002), kindly provided by Joseph Bruton (personal communication), was used to constrain the values of τ_{serca} and $\tau_{trc,on}$ by fitting the Ca^{2+} imaging curves in Abbate et al. (2002) with exponentials, yielding a lumped time constant ($\sim \tau_{serca} + \tau_{trc,on}$) in the order of 40–60 ms for the removal of Ca^{2+} from the myoplasm. Further constraints on the model parameters were obtained by fitting the slope of muscle activation (tension) as a function of stimulation frequency to experimental data. For example, Fig. 6 in Browne (1976) shows a sigmoidal force–frequency relationship, where there is a 1 to 8 ratio between 20 Hz activation and 120 Hz activation, a feature that may be captured in the present model by modifying the value of τ_{RyR}, which directly affects the dynamics of the facilitation process defined by (5), and effectively changes the slope of the sigmoidal force–frequency relationship (as shown in Fig. 2). To this author's knowledge, this is the first time such a link has been suggested, at least from a modeling perspective. Table 1 shows a list of the parameters used to generate the simulation figures.

Catch-like effect in slow muscle fibers

Figure 3a shows the muscle activation level, $\overline{\varphi_{trc}}$, as it varies in time during stimulation at various frequencies. Parameters were as listed in Table 1. In each case, the larger amplitude responses were obtained by inserting an

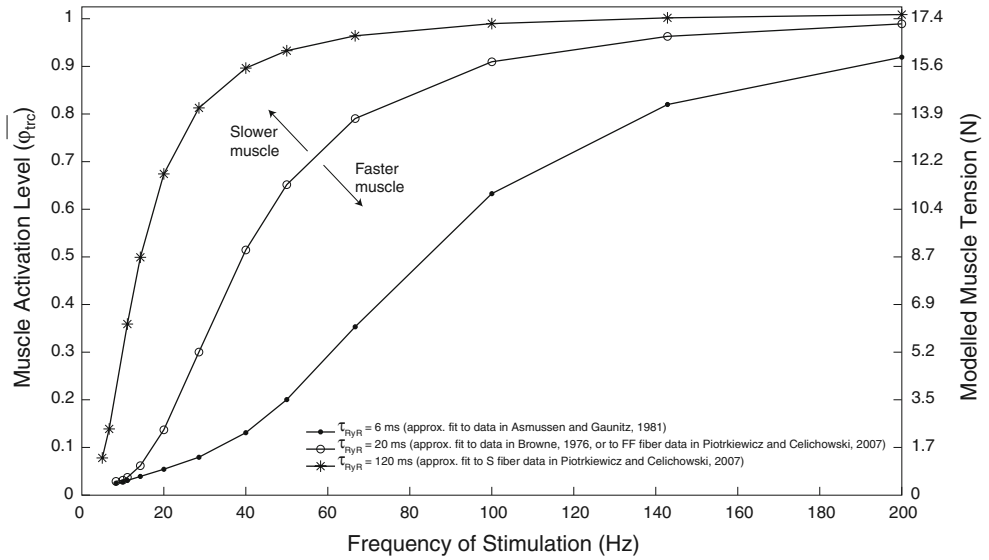

Fig. 2 Force–frequency relationship of the model. It is seen that the slope of the force–frequency relation depends on the parameter τ_{RyR}, a time constant that controls the rate of recovery of the ryanodine receptor. According to (5), the larger the value of τ_{RyR} is, the slower will the Ca^{2+} release fraction of the ryanodine receptor (ξ_{RyR}) recover to its baseline release fraction (ξ_0). The figure shows force–frequency curves for three different values of τ_{RyR}, larger values corresponding to slower muscle fibers [approximate fits to force–frequency data from Browne (1976), Asmussen and Gaunitz (1981) and Piotrkiewicz and Celichowski (2007), as indicated in figure]. Simulation parameters are listed in Table 1 and forces as in Fig. 3

Table 1 Simulation parameters

Parameter	Force–frequency (Fig. 2)	Slow fiber (Fig. 3)	Fast fiber (Fig. 4)	Ca^{2+} (Fig. 5)	Doublets (Fig. 6)	Long-term Ca^{2+} (Fig. 7)
τ_{csq}	20	20	20	20	20	20
τ_{serca}	25	40	15	15	40	40
τ_{RyR}	6–120	100	6	20	6	20
$\tau_{trc,on}$	30	20	50	40	20	20
$\tau_{trc,off}$	300	100	80	100	100	200
$\tau_{par,on}$	–	–	100	–	–	–
$\tau_{par,off}$	–	–	1,000	–	–	–
ξ_0	0.0 15	0.025	0.1	0.1	0.017	0.025
ε	0.2	0.2	0.8	0.2	0.2	0.2

All time constants are in milliseconds, and reflect the Ca^{2+} turnover rates for the corresponding partition/membrane system (and not the time constant for the individual type of channel, see text for discussion). It should be emphasized that all values are approximate and constrained according to text, but may often be varied quite substantially without deleteriously affecting the overall dynamics of the system, thus allowing for great flexibility when tuning the model to particular muscle types

extra action potential 10 ms after the beginning of the spike train, which was otherwise held constant during the experiment. This is the same activation protocol that was used by Burke et al. (1976), where the initial doublet had an interspike interval (ISI) of 10 ms. A clearly defined "catch-like" effect is observed: the extra inserted spike causes the muscle to be in a heightened level of activation, which slowly converges to the unperturbed situation. The initial approximately fivefold increase of activation level observed in this simulation is in good agreement with previously published data (Burke et al. 1976; Abbate et al. 2002), where a threefold to fivefold increase in muscle force was observed. For other muscles, there are reports of a much smaller catch-like effect (Wexler et al. 1997), which in the present simulation may be obtained by changing some of the parameters as described in the following. By systematically testing various parameter settings, the present model predicts that the time to convergence is directly proportional to the time constant for the troponin dissociation rate, $\tau_{trc,off}$. The maximum activation level at steady state is directly proportional to the stimulation frequency, and its value depends strongly on

τ_{serca} and $\tau_{trc,off}$; so, muscle activation will converge to the level corresponding to the particular frequency regardless of whether starting from a "catched" or a "noncatched" situation. The height of the initial catch-like increase depends inversely on the interspike interval of the initial doublet (see below) and on the baseline release efficiency, ξ_0, but is directly proportional to the release efficiency modifier, ε. For example, by only changing the parameters $\xi_0 = 0.04$ and $\tau_{serca} = 20$, a situation similar to that shown in Fig. 3 is obtained but with only an initial threefold catch-like increase, increasing ξ_0 further to $\xi_0 = 0.1$ leads to only a twofold increase, and so on. To evaluate the usefulness of this "activation-based" analysis, the values of $\overline{\varphi_{trc}}$ obtained for Fig. 3a were inserted into different muscle force models, as shown in Fig. 3b. One muscle force formula derived from Nielsen (2002a) has the following form:

$$F = \frac{N_{tot} k_B T \overline{\varphi_{trc}}}{bA}\left(\frac{b^2}{2L} - \frac{b}{4} + \frac{L}{4}\left(\frac{1}{1 - b/L} - 1\right)\right) \quad (7)$$

where N_{tot} is the total number of myosin–actin crossbridges involved in a given cross-section of muscle, k_B is Boltzmann's constant, T is temperature in Kelvin (here 310 K), A is the persistence length, b is the stepping length of myosin [$\sim$5.3 nm according to Kitamura et al. (1999)] and L is the unfolded length of the polymer [for a derivation of A and L, the reader is referred to Marko and Siggia (1995)]. For simplicity, only the isometric case is shown here, but the more general solution that includes nonzero contraction velocities given by Nielsen (2002a) applies equally well. Very similar results (not shown here) were obtained using a muscle force model based on a simple sigmoidal force–calcium relationship of the type described by Ebashi and Endo (1968), with the form:

$$F = F_{max}\left(\frac{2}{1 + \exp(-5\overline{\varphi_{trc}})} - 1\right) \quad (8)$$

where F_{max} is the maximal force that may be exerted by the muscle.

Note that, comparing the time course of muscle forces in Fig. 3b with the activation curves in Fig. 3a, it is seen that the form of the curves are almost identical; so, for the remainder of this work, only the activation curves will be considered.

Catch-like effect in fast muscle fibers

In fast muscle fibers, the "catch-like" effect is much less pronounced and only consists of a short-term increase in the perturbed fiber's activation level. A simulation of the fast fiber's activation levels is shown in Fig. 4; as before, the interspike interval of the initial doublet was 10 ms.

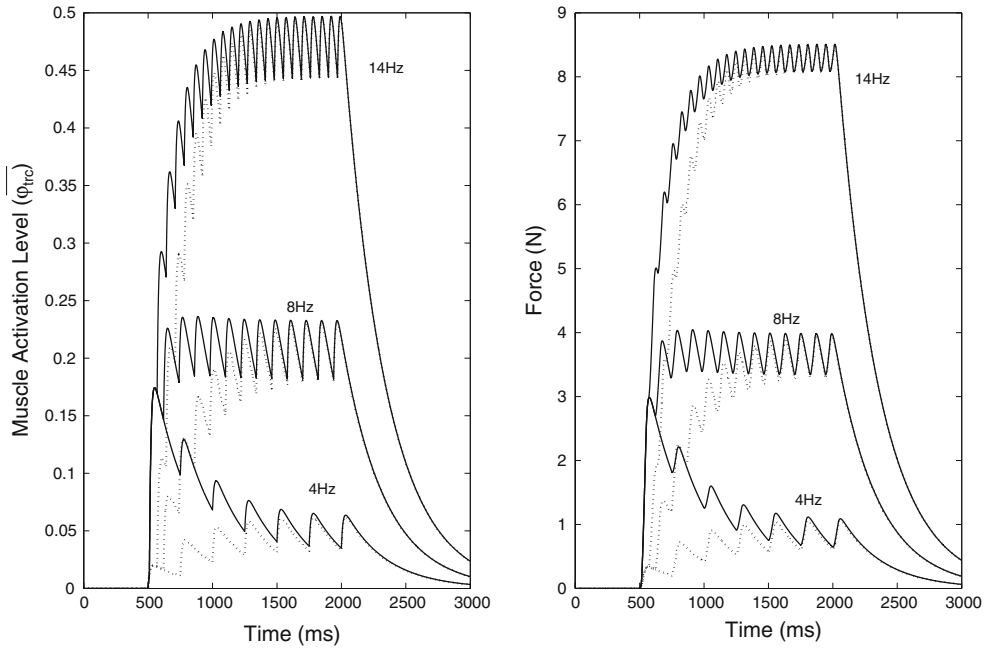

Fig. 3 Simulation of slow fiber activation dynamics using model with parameters as indicated in Table 1. **a** *Lines* show muscle activation levels during stimulations with (*full line*) and without (*dotted line*) a catch-inducing doublet (10 ms ISI) preceding a continuous stimulation at different fixed frequencies (4, 8 and 14 Hz as shown in the graph). **b** A running average of $\overline{\varphi_{trc}}$ with a window size of 40 ms was used to calculate muscle forces corresponding to the activation levels in **a**, using (7). Muscles were in all cases assumed to have a radius of 5 mm, and parameters set as in Nielsen (2002a). Given the similarity between plots in **a** and **b**, activation levels will be used for the remainder of this work. Simulation parameters are listed in Table 1

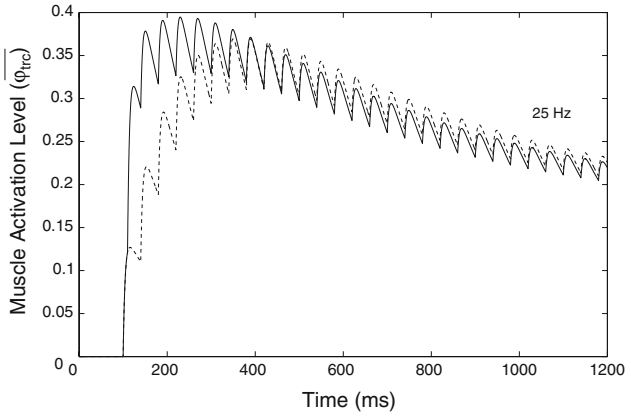

Fig. 4 Simulation of fast fiber activation dynamics using model with parameters as indicated in Table 1. *Lines* correspond to muscle activation levels with (*full line*) and without (*dashed line*) catch-inducing doublet (10 ms ISI) preceding a continuous 25 Hz stimulation

Note that the initially high activation level slowly decays and stabilizes at a long-term level that is about half the initial activation level. This rate of decay is fully determined by the ratio between the parvalbumin association and dissociation time constants ($\tau_{par,on}$ and $\tau_{par,off}$, respectively), which influences the fraction of Ca^{2+} bound to parvalbumin, φ_{par}.

Ca^{2+} transients during catch-like effect

According to recent experiments by Abbate et al. (2002), prolonged increases in force production are not necessarily correlated with increases in myoplasmic Ca^{2+}. To test whether this observation is also valid for the present model, a simulation is presented in Fig. 5 showing an attempt to reproduce the same activation criteria used by Abbate et al. (2002). For the catch-like inducing trace, a triplet with 6.5 ms interspike intervals was inserted at time 500 ms. From the upper curve (Fig. 5a), it is seen that in fact the myoplasmic Ca^{2+} very rapidly returns to the preactivation level, whereas it may be observed from Fig. 5b that the actual muscle activation, $\overline{\varphi_{trc}}$, remains elevated for several hundred milliseconds after the high-frequency burst. The prolonged force is here attributed to slow release of Ca^{2+} from troponin.

The role of doublets and missing pulses

A spike doublet inserted right at the transition between a period of low activity and one of heightened activity will bring the muscle to the increased target force almost instantaneously, compared to the case where only the frequency changes but without such a doublet. Figure 6 shows muscle activation levels during such transitions for

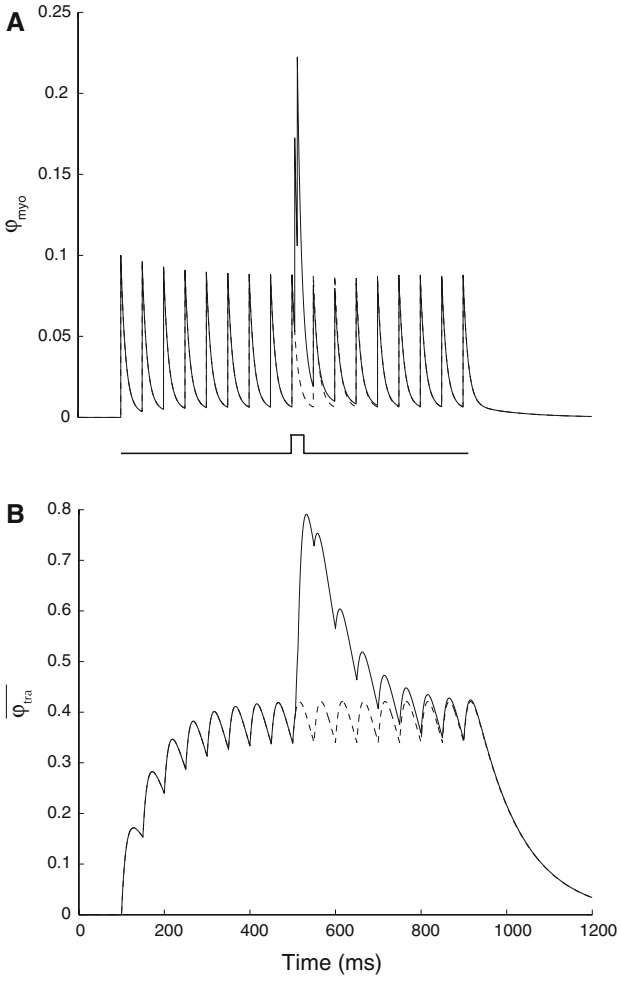

Fig. 5 Calcium transients during catch-like effect. **a** This figure shows myoplasmic Ca^{2+} following a brief high-frequency burst (three consecutive spikes at 6.5 ms interspike intervals) inserted into a regular 20 Hz spike train. *Dashed line* shows simulation results without such a burst. Note that φ_{myo} rapidly returns to the nonburst situation within 100 ms. **b** Muscle activation levels obtained with (*full line*) and without (*dashed line*) the insertion of a high-frequency burst into a regular 20 Hz spiketrain. The increased activation level, $\overline{\varphi_{trc}}$, continues for at least 300 ms after burst

different values of the interspike interval between the two spikes of the initial doublet. Controlling this interspike interval appears to be very important to fine-tune the muscle's response to correctly reach the target amplitude of the frequency change. The optimal interspike intervals to reach specified target forces are shown in Fig. 6b. This compares favorably to the experimentally observed relation between work and minimal interval reported by Maton and Bouisset (1975): as the work increases, the optimal interspike interval decreases. Further simulations (not shown) reveal that too short interspike intervals lead to overshooting of the target, and conversely, the absence of a spike will have the opposite effect, namely to immediately reduce muscle activation to the lowered target force

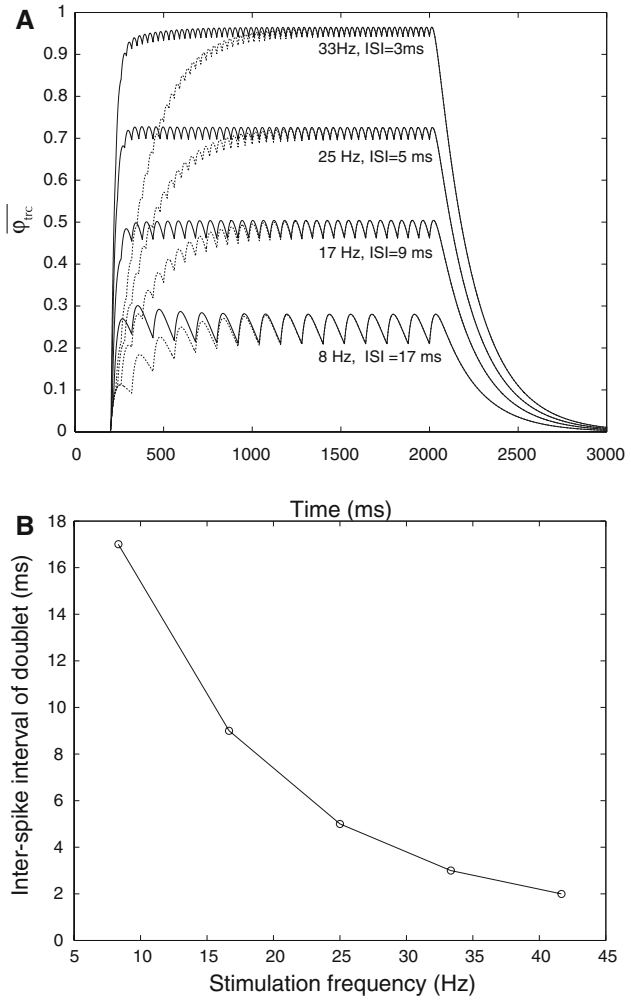

Fig. 6 Defining optimal interspike intervals for doublets. **a** Resulting activation levels of slow twitch muscles when preceded (*full line*) or not preceded (*dashed line*) by doublets of variable interspike intervals. Note that high stimulation frequencies lead to higher target forces, but require shorter "optimal" doublet interspike intervals, as shown in **b**, in accordance with experimental results reported by Maton and Bouisset (1975)

compared to the case with just a simple change in frequency. It should be noted that the shortest interspike intervals used here (3 and 5 ms) might well be unrealistically short from a physiological point of view but are nevertheless included here to fully characterize the curve in Fig. 6b. Depending on muscle type, the actual "optimal" interspike intervals will vary.

Long-term effects of tetanic activation

The present model assumes that the amount of intracellular calcium remains constant during normal stimulation. However, persistent increases of resting cytosolic (myoplasmic) [Ca^{2+}] and higher Ca^{2+} transients during pulses are features that have been observed following tetanic potentiations in muscles stimulated with adrenaline (Decostre et al. 2000). Such changes in the Ca^{2+} balance can easily be implemented within the scope provided by the present model simply by relaxing the requirement to maintain a constant φ_{tot}. Figure 7 shows the long-term effect on muscle activation of suddenly increasing the total amount of available Ca^{2+}. The question remains as to where this extra calcium comes from (the model yields no answers on this point), but one possibility is that additional extracellular calcium could gain access to the myoplasm via a delayed slow opening of the L-type DHPR Ca^{2+} channel (see, e.g., Feldmeyer et al. 1990; Garcia et al. 1990; Shtifman et al. 2004). This could be one role for the retrograde coupling in which RyR channels modulate the characteristics of the L-type Ca^{2+} current flowing through the DHPR ion-channel (see, e.g., Nakai et al. 1996; Dulhunty et al. 2002). The results on Fig. 7 have some similarity to an effect known as *post-tetanic potentiation*, especially considering the prolonged and persistent increase in muscle activation following a tetanus (Fig. 7a), an increase that is evident even if only single twitches are considered over long times (Fig. 7b). A prolonged increase in [Ca^{2+}] as described here cannot by itself directly induce the relatively large increase in force observed during PTP, but it might be involved in triggering the phosphorylation of myosin light chains, generally accepted to be the event leading to PTP as such [reviewed in Abbate et al. (2001)]. Phosphorylation of proteins in general causes long-term and persistent changes in the way that the involved proteins respond to their environment, potentially changing binding affinities, mechanical constraints, reaction rates, etc. Thus, to further improve and develop the model presented here, it would be interesting to include a formalization of the chemical and mechanical consequences of phosphorylation on the involved molecules, a topic which at present falls outside the scope of this study focusing on the role of Ca^{2+} dynamics in the stimulation frequency-dependent responses of muscles.

Conclusion

To understand the origin of a variety of stimulation frequency-dependent muscle responses such as the catch-like effect and tetanic potentiation, a simple mathematical model has been developed that captures the essential dynamics while keeping the number of parameters to a minimum (only seven parameters are used for slow-twitch fibers, and nine for fast twitch fibers). The approach taken here is based on an analysis of the way that Ca^{2+} resources are allocated within the muscle cell, focusing in particular on the flow of Ca^{2+} between different sources and sinks that are present in muscle cells. Figure 1 gives an overview

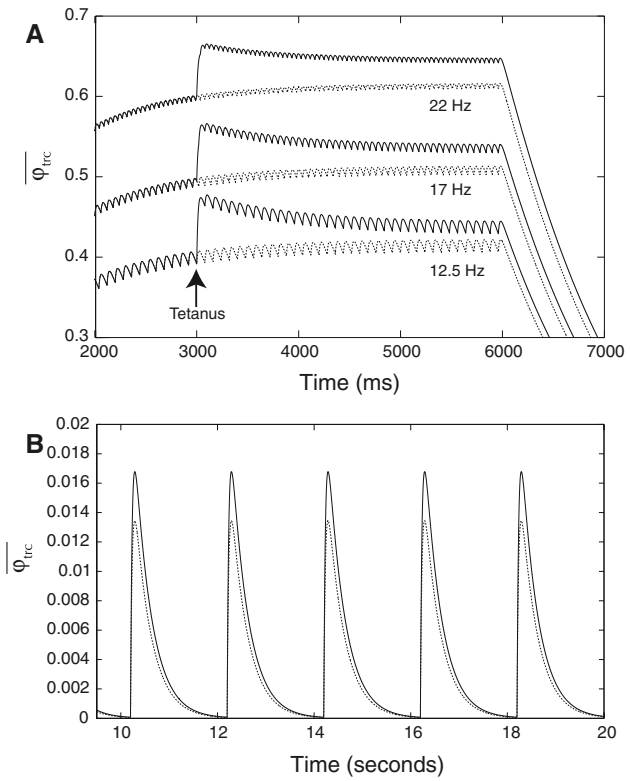

Fig. 7 Long-term effects of tetanic stimulation. **a** This figure shows the effects on muscle activation levels of suddenly increasing the total available Ca^{2+} within the cell at the time marked "tetanus." The total amount of Ca^{2+} in the cell was increased by a fraction 0.05. *Dashed lines* correspond to the normal muscle activation levels without the included tetanus. At the three frequencies investigated, a very prolonged increase in force is observed and is due to a shift in the the long-term activation level that normally follows continuous stimulations at a fixed frequency. **b** At very low (nonfusing) stimulation frequencies, individual twitches may be identified and also here an enhanced and persistent twitch activation level is observed following an increase of total Ca^{2+} by a fraction 0.25

of the main Ca^{2+} sinks and sources used in this model. To ensure a complete separation of force-producing mechanisms from the muscle cell's Ca^{2+} dynamics, the fraction of Ca^{2+} bound to troponin C was used as a direct measure of muscle activation.

From these results, it is concluded that the differences in frequency-dependent muscle responses observed between fast and slow muscle fibers can be accounted for by considering the following parameters: differences in the Ca^{2+} binding and dissociation times from troponin C ($\varphi_{tro,on}$ and $\varphi_{tro,off}$), differences in the DHPR–RyR interaction dynamics controlling Ca^{2+} release from the sarcoplasm (modulated by ε, ξ_0 and τ_{RyR}), the efficiency of sarco(endo)plasmic Ca^{2+} ATPase (SERCA) pumps (φ_{serca}) and the absence of parvalbumin in slow twitch fibers. As stated in the "Results," each of these parameters has very specific effects on the dynamics of the catch-like effect. Furthermore, it seems that additional parameters like the time constants of calsequestrin (τ_{csq}) and the ryanodine receptor (τ_{RyR}), although important for the overall dynamics of the system, are not essential for the development of the catch-like effect, nor for PTP. Intriguingly, the parameter τ_{RyR} seems to have a role in affecting the slope of the force–frequency relation in the muscle. Thus, if one knows the force–frequency relation of a particular muscle under study, the parameter τ_{RyR} provides a very useful regulatory knob that may be used to fit the force–frequency response of the present model very precisely to a given muscle under experimental scrutiny (see Fig. 2). Although perhaps not an issue in most skeletal muscle studies, this observation might be relevant for understanding cardiac muscle dysfunction, as there is now evidence that regional alterations in the force–frequency relation is the underlying cause of some heart failures (Mulieri et al. 1992, 2005), and some evidence points to differences in the expression of RyR as the main culprit (Brillantes et al. 1992). This is a further evidence to the generality of the model presented here.

Overall, the modeled results are in good agreement with the original experiments reported by Burke et al. (1970, 1976), and also compare favorably with recent experiments showing that the prolonged increase in force characteristic of the catch-like effect, as reported by Abbate et al. (2002), is not accompanied by a sustained increase in free myoplasmic Ca^{2+}. As shown in Fig. 2, it was also relatively easy to obtain force–frequency relations that matched experiments quite accurately (Browne 1976; Asmussen and Gaunitz 1981; Piotrkiewicz and Celichowski 2007). Good qualitative agreement was also obtained between the modeled results and early experiments by Maton and Bouisset (1975), which show that the duration of the interspike interval in the initial doublet strongly influences the resulting amplitude of the catch-like effect.

To account for the long-term effects of tetanic stimulation, one additional assumption is needed pertaining to the role of frequency-dependent interactions in and between ion-channels in the triad junction. It is suggested that tetanic stimulation leads to an extra influx of Ca^{2+} from extracellular sources through the DHPR channel, resulting in an increase of the total calcium available within the muscle cell. This increase shifts the Ca^{2+} equilibrium point and directly results in a prolonged increase in muscle activation that lasts as long as the extra calcium is available.

The simulation results presented here indicate that the catch-like effect is part of a fast response system designed to bring the muscle to a target force much faster than would otherwise be possible if only pulse frequency changes were applied. To function properly, this would entail that a certain degree of preprogramming exists already at the motor cortical and spinal levels, so that expected target

forces are predicted in advance of the actual movements taking place. Direct evidence related to the role of spike doublets with respect to preprogramming of movement is notoriously difficult to obtain, although there are several experiments that indicate that such a relationship might exist both at the motor cortical (Chen et al. 1996) and at the motor neuronal levels (Maton and Bouisset 1975; Garland and Griffin 1999; Søgaard et al. 2001). The generation of ballistic movements through forward modeling of movements is a well-documented and efficient mode of function [see, e.g., the case reports by Taub et al. (1975) and Rothwell et al. (1982)], but there is still some debate regarding to what extent sensorimotor feedback might also play a role in the regulation of preprogrammed movement [see, e.g., the review by Desmurget and Grafton (2000)]. Recent models of the mechanical properties of muscle spindles have shown that even sensorimotor feedback could in principle be under feedforward control by fine-tuning the activities in both the α and γ motoneuronal systems in such a way as to cancel only expected reafference feedback (Nielsen 2002b). To fully take advantage of all these frequency-dependent effects would require precise control of spatiotemporal firing-pattern sequences like those discussed by Nielsen (2003), and is the subject of a future study.

References

Abbate F, van der Velden J, Stienen G, de Haan A (2001) Post-tetanic potentiation increases energy cost to a higher extent than work in rat fast skeletal muscle. J Muscle Res Cell Motil 22:703–710

Abbate F, Bruton J, de Haan A, Westerblad H (2002) Prolonged force increase following a high-frequency burst is not due to a sustained elevation of $[Ca^{2+}]_i$. Am J Physiol Cell Physiol 283:C42–C47

Alberts B, Johnson A, Lewis J, Raff M, Roberts K, Walther P (2002) Molecular biology of the cell, 4th edn. Garland Science, New York

Asmussen G, Gaunitz U (1981) Mechanical properties of the isolated inferior oblique muscle of the rabbit. Pflugers Arch 392:183–190

Beard N, Laver D, Dulhunty A (2004) Calsequestrin and the calcium release channel of skeletal and cardiac muscle. Prog Biophys Mol Biol 85:33–69

Binder-Macleod S, Barker C III (1991) Use of a catchlike property of human skeletal muscle to reduce fatigue. Muscle Nerve 14:850–857

Binder-Macleod S, Kesar T (2005) Catchlike property of skeletal muscle: recent findings and clinical implications. Muscle Nerve 31:681–693

Bobet J, Stein R (1998) A simple model of force generation by skeletal muscle during dynamic isometric contractions. IEEE Trans Biomed Eng 45(8):1010–1016

Bottinelli R, Reggiani C (2000) Human skeletal muscle fibres: molecular and functional diversity. Prog Biophys Mol Biol 73:195–262

Brandt P, Cox R, Kawai M (1980) Can the binding of Ca^{2+} to two regulatory sites on troponin C determine the steep pca/tension relationship of skeletal muscle? Proc Natl Acad Sci USA 77(8):4717–4720

Brillantes A-M, Allen P, Takahashi T, Izumo S, Marks A (1992) Differences in cardiac calcium release channel (ryanodine receptor) expression in myocardium from patients with end-stage heart failure caused by ischemic versus dilated cardiomyopathy. Circ Res 71:18–26

Browne J (1976) The contractile properties of slow muscle fibres in sheep extraocular muscle. J Physiol 254:535–550

Burke R, Rudomin P, Zajac F (1970) Catch property in single mammalian motor units. Science 168(3927):122–124

Burke R, Rudomin P, Zajac F (1976) The effect of activation history on tension production by individual muscle units. Brain Res 109:515–529

Cannell M (1986) Effect of tetanus duration on the free calcium during the relaxation of frog skeletal muscle fibres. J Physiol 376:203–218

Celio M, Heizmann W (1982) Calcium-binding protein parvalbumin is associated with fast contracting muscle fibres. Nature 297:504–506

Chen W, Zhang J, Hu G, Wu C (1996) Electrophysiological and morphological properties of pyramidal and nonpyramidal neurons in the cat motor cortex in vitro. Neuroscience 73(1):39–55

Cho J, Oh Y, Park K, Yu J-R, Choi K, Shin J-Y, Kim D, Park W, Hamada T, Kagawa H, Maryon E, Bandyopadhyay J, Ahnn J (2000) Calsequestrin, a calcium sequestering protein localized at the sarcoplasmic reticulum, is not essential for body-wall muscle function in *Caenorhabditis elegans*. J Cell Sci 113:3947–3958

Chou C, Hannaford B (1992) Dual stable point model of muscle activation and deactivation. Biol Cybernet 66:511–523

Chou L, Ding J, Wexler A, Binder-Macleod S (2005) Predicting optimal electrical stimulation for repetitive human muscle activation. J Electromyogr Kinesiol 15:300–309

Collins J (1991) Myosin light chains and troponin C: structural and evolutionary relationships revealed by amino acid sequence comparisons. J Muscle Res Cell Motil 12:3–25

Collins J, Potter J, Horn M, Wilshire G, Jackman N (1973) The amino acid sequence of rabbit skeletal muslce troponin C: gene replication and homology with calcium-binding proteins from carp and hake muscle. FEBS Lett 36(3):268–272

Decostre V, Gillis J, Gailly P (2000) Effect of adrenaline on the post-tetanic potentiation in mouse skeletal muscle. J Muscle Res Cell Motil 21:247–254

Desmurget M, Grafton S (2000) Forward modeling allows feedback control for fast reaching movements. Trends Cognit Sci 4(11):423–431

Ding J, Binder-MacLeod S, Wexler A (1998) Two-step, predictive, isometric force model tested on data from human and rat muscles. J Appl Physiol 85(6):2176–2189

Ding J, Wexler A, Binder-MacLeod S (2000) Development of a mathematical model that predicts optimal muscle activation patterns by using brief trains. J Appl Physiol 88:917–925

Ding J, Wexler A, Binder-Macleod S (2002) A mathematical model that predicts the force–frequency relationship of human skeletal muscle. Muscle Nerve 26:477–485

Dulhunty A, Haarmann C, Green D, Laver D, Board P, Casarotto M (2002) Interactions between dihydropyridine receptors and ryanodine receptors in striated muscle. Prog Biophys Mol Biol 79:45–75

Ebashi S, Endo M (1968) Calcium ion and muscle contraction. Prog Biophys Mol Biol 18:123–183

Edman K (1996) Fatigue vs. shortening-induced deactivation in striated muscle. Acta Physiol Scand 156:183–192

Feldmeyer D, Melzer W, Pohl B, Zöllner P (1990) Fast gating kinetics of the slow Ca^{2+} current in cut skeletal muscle fibres of the frog. J Physiol 425:347–367

Fill M, Copello J (2002) Ryanodine receptor calcium release channels. Physiol Rev 82:893–922

Franzini-Armstrong C (1999) The sarcoplasmic reticulum and the control of muscle contraction. FASEB J 13:S266–S270

Franzini-Armstrong C, Ferguson D (1985) Density and disposition of Ca^{2+}–ATPase in sarcoplasmic reticulum membrane as determined by shadowing techniques. Biophys J 48(4):607–615

Ganitkevich V (1999) Clearance of large Ca^{2+} loads in a single smooth muscle cell: examination of the role of mitochondrial Ca^{2+} uptake and intracellular pH. Cell Calcium 21(1):29–42

Garcia J, Avila-Sakar A, Stefani E (1990) Repetitive stimulation increases the activation rate of skeletal muscle Ca^{2+} currents. Pflugers Arch 416:210–212

Garland S, Griffin L (1999) Motor unit double discharges: statistical anomaly or functional entity. Can J Appl Physiol 24(2):113–130

Geeves M, Lehrer S (2002) Modeling thin filament cooperativity. Biophys J 82:1677–1679

Gilchrist J, Palahniuk C, Bose R (1997) Spectroscopic determination of sarcoplasmic reticulum Ca^{2+} uptake and Ca^{2+} release. Mol Cell Biochem 172:159–170

Gordon A, Ridgway E (1987) Extra calcium on shortening in barnacle muscle. J Gen Physiol 90:321–340

Gurrola G, Arvalo C, Sreekumar R, Lokuta A, Walker J, Valdivia H (1999) Activation of ryanodine receptors by imperatoxin A and a peptide segment of the II–III loop of the dihydropyridine receptor. J Biol Chem 274(12):7879–7886

Hannaford B (1990) A nonlinear model of the phasic dynamics of muscle activation. IEEE Trans Biomed Eng 37(11):1067–1075

Higgins E, Cannell M, Sneyd J (2006) A buffering SERCA pump in models of calcium dynamics. Biophys J 91:151–163

Hill A (1938) The heat of shortening and the dynamic constants of muscle. Proc Roy Soc B Biol Sci 126:136–195

Huxley A, Simmons R (1971) Proposed mechanism of force generation in striated muscle. Nature 233:533–538

Johnson J, Charlton S, Potter J (1979) A fluorescence stopped flow analysis of Ca^{2+} exchange with troponin C. J Biol Chem 254:3497–3502

Jorgensen A, Kalnins V, MacLennan D (1979) Localization of sarcoplasmic reticulum proteins in rat skeletal muscle by immunofluorescence. J Cell Biol 80:372–384

Jorgensen A, Shen A, MacLennan D, Tokuyasu K (1982) Ultrastructural localization of the $Ca^{2+} + Mg^{2+}$-dependent ATPase of sarcoplasmic reticulum in rat skeletal muscle by immunoferritin labeling of ultrathin frozen sections. J Cell Biol 92:409–416

Jorgensen A, Shen A, Campbell K, MacLennan D (1983) Ultrastructural localization of calsequestrin in rat skeletal muscle by immunoferritin labeling of ultrathin frozen sections. J Cell Biol 97:1573–1581

Kebaetse M, Lee S, Binder-MacLeod S (2001) A novel stimulation pattern improves performance during repetitive dynamic contractions. Muscle Nerve 24:744–752

Kebaetse M, Lee S, Johnston T, Binder-MacLeod S (2005) Strategies that improve paralyzed human quadriceps femoris muscle performance during repetitive nonisometric contractions. Arch Phys Med Rehabil 86:2157–2164

Kerrick W, Secrist D, Coby R, Lucas S (1976) Development of difference between red and white muscles in sensitivity to Ca^{2+} in the rabbit from embryo to adult. Nature 260:440–441

Kitamura K, Tokunaga M, Iwane A, Yanagida T (1999) A single myosin head moves along an actin filament with regular steps of 5.3 nanometres. Nature 397:129–134

Kugler G, Weiss R, Flucher B, Grabner M (2004) Structural requirements of the dihydropyridine receptor α_{1S}II–III loop for skeletal-type excitation-contraction coupling. J Biol Chem 279(6):4721–4728

Lee J, Westerblad H, Allen D (1991) Changes in tetanic and resting $[Ca^{2+}]_i$ during fatigue and recovery of single muscle fibres from *Xenopus laevis*. J Physiol 433:307–326

Marko J, Siggia E (1995) Stretching DNA. Macromolecules 28:8759–8770

Maton B, Bouisset S (1975) Motor unit activity and preprogramming of movement in man. Electroencephalogr Clin Neurophysiol 38:658–660

Mogami H, Tepikin A, Petersen O (1998) Termination of cytosolic Ca^{2+} signals: Ca^{2+} reuptake into intracellular stores is regulated by the free Ca^{2+} concentration in the store lumen. EMBO J 17(2):435–442

Mourselas N, Granat M (1998) Evaluation of patterned stimulation for use in surface functional electrical stimulation systems. Med Eng 20:319–324

Mulieri L, Hasenfuss G, Leavitt B, Allen P, Alpert N (1992) Altered myocardial force–frequency relation in human heart failure. Circulation 85:1743–1750

Mulieri L, Tischler M, Martin B, Leavitt B, Ittleman F, Alpert N, LeWinter M (2005) Regional differences in the force–frequency relation of human left ventricular myocardium in mitral regurgitation: implication for ventricular shape. Am J Physiol Heart Circ Physiol 288:H2185–H2191

Murray B, Ohlendieck K (1998) Complex formation between calsequestrin and the ryanodine receptor in fast- and slow-twitch rabbit skeletal muscle. FEBS Lett 429:317–322

Nakai J, Dirksen R, Nguyen H, Pessah I, Beam K, Allen P (1996) Enhanced dihydropyridine receptor channel activity in the presence of ryanodine receptor. Nature 380:72–75

Nielsen B (2002a) Entropic elasticity in the generation of muscle force—a theoretical model. J Theor Biol 219(1):99–119

Nielsen B (2002b) The role of muscle spindles in constraining motor control. Neurocomputing 44:943–949

Nielsen B (2003) Sequence learning in differentially activated dendrites. Netw Comput Neural Syst 14:189–209

Nielsen B (2004) Towards bridging the gap from molecular forces to the movement of organisms. Biochem Soc Trans 32(5):694–696

Otazu G, Futami R, Hoshimiya N (2001) A muscle activation model of variable stimulation frequency response and stimulation history, based on positive feedback in calcium dynamics. Biol Cybernet 84:193–206

Patel J, McDonald K, Wolff M, Moss R (1997) Ca^{2+} binding to troponin c in skinned skeletal muscle fibers assessed with caged Ca^{2+} and a Ca^{2+} fluorophore. J Biol Chem 272(9):6018–6027

Peinelt C, Apell H-J (2004) Time-resolved charge movements in the sarcoplasmatic reticulum Ca–ATPase. Biophys J 86:815–824

Piotrkiewicz M, Celichowski J (2007) Tetanic potentiation in motor units of rat medial gastrocnemius. Acta Neurobiol Exp 67:35–42

Potter J, Gergely J (1975) The calcium and magnesium binding sites on troponin and their role in the regulation of myofibrillar adenosine triphosphatase. J Biol Chem 250(12):4628–4633

Protasi F, Paolini C, Nakai J, Beam K, Franzini-Armstrong C, Allen P (2002) Multiple regions of ryr1 mediate functional and structural interactions with α_{1S}-dihydropyridine receptors in skeletal muscle. Biophys J 83:3230–3244

Ridgway E, Gordon A (1975) Muscle activation: effects of small length changes on calcium release in single fibers. Science 189:881–884

Ridgway E, Gordon A, Martyn D (1983) Hysteresis in the force–calcium relation in muscle. Science 219:1075–1077

Rothwell J, Traub M, Day B, Obeso J, Thomas P, Marsden C (1982) Manual motor performance in a deafferented man. Brain 105:515–542

Shimada Y, Ito H, Matsunaga T, Misawa A, Kawatani M, Itoi E (2006) Reduction of muscle fatigue by catchlike-inducing

intermittent electrical stimulation in rat skeletal muscle. Biomed Res 27(4):183–189

Shtifman A, Paolini C, Lpez J, Allen P, Protasi F (2004) Ca^{2+} influx through α_{1S} DHPR may play a role in regulating Ca^{2+} release from ryr1 in skeletal muscle. Am J Physiol Cell Physiol 286:C73–C78

Simpson J (1969) Terminology of electromyography. Electroencephalogr Clin Neurophysiol 26:224–226

Søgaard K, Sjøgaard G, Finsen L, Olsen H, Christensen H (2001) Motor unit activity during stereotyped finger tasks and computer mouse work. J Electromyogr Kinesiol 11:197–206

Solovyova N, Veselovsky N, Toescu E, Verkhratsky A (2002) Ca^{2+} dynamics in the lumen of the endoplasmic reticulum in sensory neurons: direct visualization of Ca^{2+}- induced Ca^{2+} release triggered by physiological Ca^{2+} entry. EMBO J 21(4):622–630

Stein R, Parmiggiani F (1979) Optimal motor patterns for activating mammalian muscle. Brain Res 175:372–376

Stein R, Bobet J, Oğuztöreli M, Fryer M (1988) The kinetics relating calcium and force in skeletal muscle. Biophys J 54:705–717

Takekura H, Flucher B, Franzini-Armstrong C (2001) Sequential docking, molecular differentiation, and positioning of T-tubule/SR junctions in developing mouse skeletal muscle. Dev Biol 239:204–214

Talonen P, Baer G, Häkkinen V, Ojala J (1990) Neurophysiological and technical considerations for the design of an implantable phrenic nerve stimulator. Med Biol Eng Comput 28:31–37

Taub E, Goldberg I, Taub P (1975) Deafferentiation in monkeys—pointing at a target without visual feedback. Exp Neurol 46(1):178–186

Tsodyks M, Markram H (1997) The neural code between neocortical pyramidal neurons depends on neurotransmitter release probability. Proc Natl Acad Sci USA 94:719–723

Tsodyks M, Pawelzik K, Markram H (1998) Neural networks with dynamic synapses. Neural Comput 10:821–835

van Eerd J-P, Takahashi K (1975) The amino acid sequence of bovine cardiac troponin-C. Comparison with rabbit skeletal troponin-C. Biochem Biophys Res Commun 64(1):122–127

Westerblad H, Allen D (1993) The contribution of $[Ca^{2+}]_i$ to the slowing of relaxation in fatigued single fibres from mouse skeletal muscle. J Physiol 468:729–740

Wexler A, Ding J, Binder-Macleod S (1997) A mathematical model that predicts skeletal muscle force. IEEE Trans Biomed Eng 44(5):337–348

Winters J (1995) How detailed should muscle models be to understand multi-joint movement coordination? Hum Mov Sci 14(4/5):401–442